

Direct-Hydrocarbon Proton-Conducting SOFCs

Subjects: Electrochemistry

Contributor: Fan Liu

Solid oxide fuel cells (SOFCs) are promising and rugged solid-state power sources that can directly and electrochemically convert the chemical energy into electric power. Direct-hydrocarbon SOFCs eliminate the external reformers; thus, the system is significantly simplified and the capital cost is reduced. To reduce operating temperatures of SOFCs, intermediate-temperature proton-conducting SOFCs (P-SOFCs) are being developed as alternatives, which give rise to superior power densities, coking and sulfur tolerance, and durability. Due to these advances, there are growing efforts to implement proton-conducting oxides to improve durability of direct-hydrocarbon SOFCs.

Keywords: proton-conducting oxides ; direct-hydrocarbons SOFCs ; coking ; durability

1. Introduction

Fossil energy sources, including coal, oil, and natural gas, are currently accounting for >80% of the global energy consumption. The rapid growth in fossil fuel extraction, transportation, and consumption is leading to significant anthropogenic climate change and global warming accompanied by the principal CO₂ emission ^{[1][2]}. Additionally, fossil fuels are not sustainable, and their depletion has been identified as a near-future challenge. Therefore, great efforts have been devoted to ensuring a global economy transition to more efficient utilization of fossil fuels and a low-carbon future ^[3].

Solid oxide fuel cells (SOFCs) have stimulated great interest in highly efficient energy conversion ^[4]. As electrochemical energy conversion devices, SOFCs can directly and electrochemically convert the chemical energy stored in fuels into clean electric power without the limitation of the Carnot cycle, which, in turn, leads to higher energy conversion efficiency (~60%) than traditional combustion engines ^[5]. For example, gas turbines are applied to produce electricity from coal or natural gas using the intermediary steam with lower energy efficiency ranging from 30–40% ^[6]. Hydrogen is considered as the cleanest fuel, leaving only water as the product, while it is not naturally abundant, and there are many complications in its production, transportation, and storage ^[7]. Hydrocarbons could offer several attractive advantages over hydrogen, including higher volumetric energy storage density (10.05 kJ/L for hydrogen (LHV) and 36.4 kJ/L for natural gas) and lower transportation cost. For example, in the USA, natural gas or propane is usually distributed through railroad, truck, tanker ship, or pipelines into urban areas. Direct-hydrocarbon SOFCs are, therefore, one of the most promising power sources, which eliminates the fuel processor units and could be integrated into the current power grid, drastically enhancing energy conversion efficiency and reducing emissions.

The SOFC anode, which functions as the catalyst for reforming fuel streams and the electrode for charge transfer, is critical for high-performing direct-hydrocarbon SOFCs. The current SOFC anode is typically a composite of ceramic and metal (i.e., cermet) that exhibits mixed ionic and electronic conduction. For instance, the YSZ-Ni cermet is widely used as the anode for oxygen-ion SOFCs (O-SOFCs) because of its excellent catalytic activities and high electronic conductivity ^[8]. Unfortunately, Ni is vulnerable when exposed to hydrocarbon fuels as it is kinetically favorable for carbon deposition. Additionally, YSZ-Ni anodes are more prone to coking and sulfur poisoning because the relatively acidic surface of YSZ could not contribute to coke mitigation ^{[9][10][11]}. Furthermore, the YSZ-Ni cermet requires an operating temperature of >700 °C, which could thermodynamically favor the coking ascribed to the pyrolysis of hydrocarbons ^[12]. Since Ni-based anodes are not perfect for working under hydrocarbons, developing Ni-free or oxide-based anodes are emerging approaches to enhancing the durability of direct-hydrocarbon SOFCs ^[13]. Despite Ni-free anodes delivering good fuel cell performances under hydrocarbon fuels ^[14], Ni-free anodes are still far away from commercialization and the cell configuration is limited to electrolyte-supported SOFCs. Furthermore, Ni-free anodes need a higher operating temperature (>800 °C) to obtain considerable catalytic activities, and thus the costly balance of plant (BOP) components are required. Hence, few Ni-free anodes demonstrate electro-catalytic activity and electronic conductivity that can compete with the current Ni-based anode. Therefore, robust SOFC anodes, which are catalytically active at intermediate operating temperatures, coking and sulfur-tolerant, as well as chemically stable, are essential for direct-hydrocarbon SOFCs. Proton-conducting oxides have been developed for numerous electrochemical devices because of high proton

conductivity at 300–650 °C [15][16][17][18][19]. Due to their relatively basic surface for high water-uptake capability, such oxides are recently applied as anodes for direct-hydrocarbon P-SOFCs. SOFCs with proton-conducting oxides have demonstrated excellent power density and long-term durability (>1000 h), opening a new pathway for developing durable direct-hydrocarbon P-SOFCs [20][21][22].

Comprehensive aspects of hydrocarbon-fueled SOFCs [7][23][24][25][26][27][28][29] and hydrogen-powered P-SOFCs have been summarized by many review papers [21][30][31]. However, there is still a lack of review centering on the hydrocarbon-fueled P-SOFCs [32].

2. Proton-Conducting Oxides

The state-of-the-art proton-conducting oxides are ABO₃ perovskites, including five compositional groups: yttrium-doped barium zirconate (BZY), yttrium-doped barium cerate (BCY), yttrium- and cerium-doped barium zirconates (BZCY/BCZY), and yttrium-, ytterbium, and cerium-doped barium zirconates (BCZYYb) [18][31][33][34]. Due to the relatively low activation energy of proton conduction (0.4–0.6 eV), the proton-conducting oxides exhibit practically significant proton conductivity (10⁻³–10⁻² S cm⁻¹) at intermediate operating temperatures (400–600 °C) [31][35].



The protons are produced via hydration [31], as shown in Equation (1), where Kröger–Vink notation is used to describe oxygen vacancy V_O^{••}, lattice oxygen O_O^X and proton. This defect reaction indicates oxygen vacancies are required for the formation of protons OH_O[•]; thus, oxygen vacancy concentration is normally increased by the acceptor doping to improve the proton conductivity, i.e., the substitution of the Zr⁴⁺ or Ce⁴⁺ host with trivalent dopants (e.g., Y³⁺/Yb³⁺).

In the 1980s, Iwahara et al. first recognized that BCY is a proton conductor [15]. However, it was noted that BCY is chemically unstable in the presence of water and carbon dioxide [31,36]. Their poor chemical stability hinders their practical applications and much attention has been shifted to zirconate-based proton conductors, especially BZY, due to their enhanced chemical stability [16]. However, with the increased concentration of Zr⁴⁺, its poor sintering ability tends to be a thorny issue. Additionally, BZY displays high grain boundary resistance, resulting in lower proton conductivity than BCY [31]. The researchers, therefore, developed BCZY by synergizing the benefits of both BZY and BCY, improving conductivity and stability [16]. Liu et al. demonstrated that BaCe_{0.7}Zr_{0.1}Y_{0.2}O₃ possesses improved chemical stability under 2% CO₂ and 15% H₂O atmosphere and enhanced conductivity (9 × 10⁻³ S cm⁻¹) at 500 °C [17]. The same team then pioneered a novel proton conductor, BaCe_{0.7}Zr_{0.1}Y_{0.1}Yb_{0.1}O₃ [18], leading to benchmarking proton conductivity and stability under hydrocarbons with hydrogen sulfide.

To tackle the issues associated with sintering, a sintering aid (e.g., ZnO) was added to facilitate the densification and lower the sintering temperatures, increasing the feasibility of using proton-conducting oxides for building fuel cells [37]. A variety of other sintering aids, including NiO and CuO, have also been investigated for fabricating proton-conducting oxides [38]. In 2015, Duan and O'Hayre et al. [22] applied the solid-state reactive sintering method to P-SOFCs fabrication and demonstrated P-SOFCs with remarkable performances and durability with both hydrogen and methane as fuels.

3. Unique Surface Properties of Proton-Conducting Oxides

It has been recognized that increasing the basicity of the catalyst surface can suppress coking over heterogeneous catalysts [10]. Tatsuya et al. [36] investigated the catalytic activity and coking tolerance of Ni-YSZ cermet decorated with four alkaline oxides, including MgO, CaO, SrO, and CeO. CaO was identified as the most effective in improving coking tolerance, although it slightly deteriorated the electrochemical activity of the anode. Liu et al. [37] later demonstrated that the modification of the Ni + YSZ anode with nanostructured BaO, which also has a relatively basic surface, could greatly suppress the coke formation. Density functional theory suggests that BaO is capable of absorbing and dissociating water and, thereby, enabling coke mitigation. The water-mediated carbon removal mechanism is illustrated in [Figure 1](#). (1) The basic surface of BaO promotes the dissociation of water into OH* and H* over the catalyst (* indicates the surface site of catalyst); (2) OH* absorbed on BaO will then react with carbon deposited on the Ni and produce CO* and H*. (3) CO* and H* will subsequently react with the oxygen ions at the triple phase boundary and form CO₂ and H₂O.

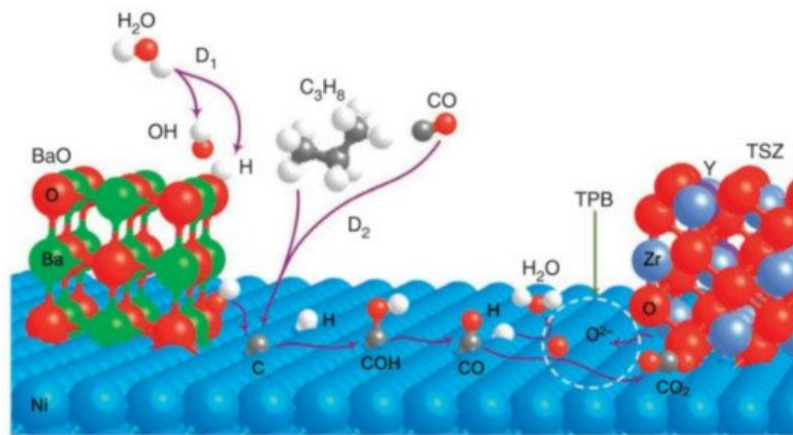


Figure 1. Proposed mechanism for water-mediated carbon removal on the anode with BaO/Ni interfaces [37].

Surface-enhanced Raman Spectroscopy (SERS) was employed to better understand the coke mitigation mechanisms of Ni-based anodes coated with BaO, BZY, and BCZYYb, respectively [38], revealing that abundant OH is absorbed on all three materials. These absorbed OH can readily react with carbon and subsequently clean coke. However, BaO can also easily react with CO_2 and form BaCO_3 , which is irreversible, leading to exacerbated SOFC performance degradation. Unlike BaO, BZY and BCZYYb are capable of regenerating OH groups, and proton-conducting oxides also have basic surfaces, indicating they could be adopted as the materials for direct-hydrocarbons/ethanol SOFCs. Liu et al. integrated BZCY-Ni with SDC as the anode of direct-ethanol SOFCs, aiming to improve its coking tolerance. They demonstrated ethanol-fueled SOFCs with a power density of 750 mW cm^{-2} at 750°C and a stable operation of 170 h. A similar water-mediated carbon removal mechanism was also proposed in this work, suggesting proton-conducting oxides (i.e., BZCY) with high water uptake capacity could accelerate the formation of C-OH intermediates and consequently enhance the carbon removal ability. Furthermore, it has been noted that proton-conducting oxides, such as BCZYYb, can also absorb CO_2 and form CO_3 groups, which can help to clean the carbon, further improving the coking tolerance [48].

4. The Rationale for Developing Direct-Hydrocarbon P-SOFCs

Although P-SOFCs are a nascent technology, they already show significant promise for highly efficient and durable power generation [19][20][22][32][34][39][40]. Compared to high-temperature oxygen-ion solid oxide cells (O-SOFCs) and low-temperature polymer electrolyte membrane fuel cells (PEMFCs) or alkaline fuel cells, P-SOFCs offer several important benefits:

- Unlike O-SOFCs (Figure 2b), as illustrated in Figure 2a, P-SOFCs can produce water in the cathode, which will not dilute the fuel stream, potentially improving the performances, enhancing fuel utilization, and reducing system complexity and cost (that is, no external condenser required for condensing water and recycling fuel), as well as enhancing overall energy efficiency [4][41].
- Intermediate-temperature P-SOFCs ($500\text{--}600^\circ\text{C}$) enable significantly higher efficiency than low temperature ($50\text{--}100^\circ\text{C}$) PEMFCs and can approach that of HT-SOFCs ($700\text{--}900^\circ\text{C}$) [42][43]. Reduced operating temperatures (versus O-SOFCs) enable the relaxing of the stack and balance-of-plant constraints, potentially lowering the cost while also improving the reliability, thermal cycling tolerance, and dynamic response.
- High hydrocarbon conversion could be achieved in the P-SOFCs because of the continuous removal of hydrogen from the anode which shifts the reaction equilibriums of steam reforming and water gas shift reaction [22].
- As shown in Figure 3 [20], the composition of P-SOFC anode gas stream lies in the thermodynamic coking boundary of the whole reaction range or just outside it. On the contrary, with increasing the fuel utilization, the composition of anode gas steam in O-SOFC moves away from the coking boundary rapidly. However, the experimental studies of P-SOFCs contradicts the thermodynamic predictions [20][22][34][40], which is due to unique surface properties of proton-conducting oxides. P-SOFCs are therefore coking and sulfur tolerant, and highly active for internal reforming.

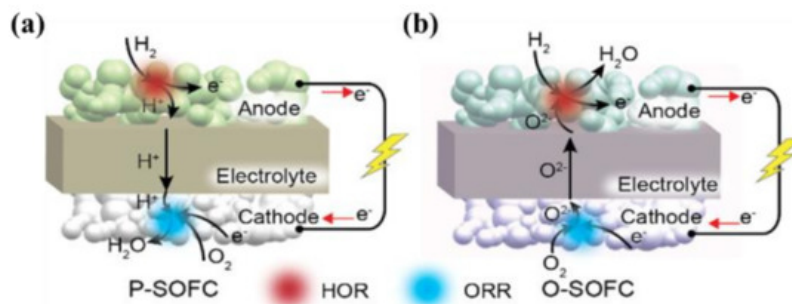


Figure 2. Schematic illustration of SOFCs with (a) a proton-conducting electrolyte; (b) an oxygen-ion conductor.

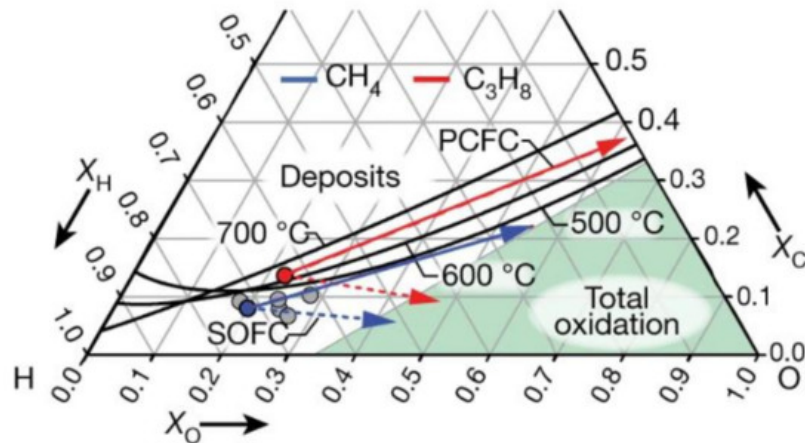


Figure 3. The ternary diagram shows the regions of equilibrium carbon formation and full oxidation. The dots indicate experimental fuel compositions. Fuel composition trajectories for propane (red) and methane (blue) are shown as solid lines for P-SOFCs (increasing current density and removing H) and dashed lines for O-SOFC (increasing current density and adding O). The end-point compositions correspond to the complete oxidation of the fuel stream to CO_2 and H_2O . ‘Deposits’ indicates the region where coking is thermodynamically favorable [20].

5. Notable Achievements on Coking-Tolerant Direct-Hydrocarbon P-SOFCs

Both P-SOFCs and O-SOFCs are capable of directly converting methane and other hydrocarbon fuels (e.g., C_2H_6 and C_3H_8) into electricity. However, coking on YSZ-Ni anode, which blocks the active sites at the triple phase boundary (TPB), results in severe degradation. This is the main obstacle to the commercialization of SOFCs. For example, Yang et al. [37] reported that the terminal voltage of O-SOFCs, when fed with dry C_3H_8 , quickly dropped to nearly zero at a current density of 500 mA cm^{-2} within the 30 min operation. There are, therefore, increasing efforts devoted to developing alternative direct-hydrocarbon fuel cells, such as P-SOFCs.

Direct-methane P-SOFCs were firstly validated by Coors in 2003. Although the current densities are too low to be commercially visible at that time, it has been demonstrated that P-SOFC shows the unique coking resistance [44]. Luo et al. [2] proved the feasibility of using propane as the fuel in P-SOFCs, achieving improved fuel cell performances [45]. Duan and O’Hayre et al. [22] employed solid state reactive sintering to fabricate P-SOFCs, tackling the manufacturing challenges arising from the poor sintering ability of proton-conducting oxides. Additionally, they deliberately designed one of the state-of-the-art triple-conducting (oxygen ion, proton, and electron hole) cathodes ($\text{BaCe}_{0.4}\text{Fe}_{0.4}\text{Zr}_{0.1}\text{Y}_{0.1}\text{O}_3$), significantly improving the performances of P-SOFCs. Direct-methane P-SOFCs with remarkable performances and a stable operation of 1400 h at 500°C were demonstrated [22]. In 2017, Liu et al. [46] reported $\text{BaCe}_{0.7}\text{Zr}_{0.1}\text{Y}_{0.2}\text{O}_{3-\delta}$ electrolyte-supported cells with a peak power density of $348.84 \text{ mW cm}^{-2}$ and 496.2 mW cm^{-2} on ethane and hydrogen, respectively at 750°C . More recently, the long-term durability of fuel-flexible P-SOFCs has been comprehensively investigated. P-SOFCs fueled with 12 different fuel streams, including hydrogen, methane, natural gas, propane, n-butane, i-butane, iso-octane, and others, exhibit a degradation rate of $<1.5\%$ per 1000 h for most fuels at $500\text{--}600^\circ\text{C}$ [20]. This entire set of durability measurements have fully validated that direct-hydrocarbon P-SOFCs are exceptionally stable. In addition to power generation, Luo et al. revealed that P-SOFCs can simultaneously generate power and produce chemicals [47]. Both outstanding fuel cell performances and syngas production rate have been achieved. The performances of hydrocarbon fueled P-SOFCs are summarized in Table 1.

Table 1. Performances of P-SOFCs fed with hydrocarbon fuels.

Year	Anode/ Electrolyte/ Cathode	Fuel	Peak Power Density (mW cm ⁻²)	Stability	Reference
2003	Ni/BCY/Pt	CH ₄	~13 at 700 °C	-	[44]
2008	Pt/BCY/Pt	C ₃ H ₈	~43 at 650 °C	-	[2]
2015	Ni-BZY20/ BZY20/ BCFZY	28.6% CH ₄ + 71.4% H ₂ O	142 at 500 °C	No degradation for 200 h, 0.15 A cm ⁻² at 500 °C	[22]
2016	Ni-BCZY/ BCZY/ PSCFM	C ₂ H ₆	120 at 650 °C 349 at 750 °C	No degradation for 200 h, 0.65 A cm ⁻² at 750 °C	[46]
2016	Ni-BCZYYb/ BCZYYb/ BCZY-LSCF	CH ₄ (3% H ₂ O)	800 at 650 °C 560 at 600 °C 320 at 550 °C	No degradation for 200 h, 0.50 A cm ⁻² at 550 °C	[47]
2016	PBMn-Ni- BCZYYb/ BCZYYb/ BCZY+ NBCCo	50% CH ₄ +50% CO ₂	560 at 700 °C	No degradation for 36 h, 1.0 A cm ⁻² at 700 °C	[39]
2017	Ni-BCZYYb/BZCY- LSGM/BZCY-LSCF	Humidified 60% CH ₄ + 40% CO ₂	210 at 500 °C 320 at 550 °C 560 at 600 °C	No degradation for 80 h, 1.5 A cm ⁻² at 650 °C	[48]
2018	Ni-BZY/ BZY/BCFZY	Natural gas with 19.5 p.p.m. H ₂ S impurity	372 at 600 °C	~10% degradation for 1000 h, 0.25 A cm ⁻² at 500 °C	[20]

Year	Anode/ Electrolyte/ Cathode	Fuel	Peak Power Density (mW cm ⁻²)	Stability	Reference
2018	Ni-BZY/BZY/ LSCF-PNM	33% CH ₄ + 33% H ₂ O + 33% N ₂	55 at 550 °C 96 at 600 °C 132 at 650 °C	No degradation for 20 h, 0.6 V at 550 °C	[49]

To improve the durability of direct-hydrocarbon O-SOFCs, proton-conducting oxides have also been used for decorating the anode of O-SOFCs [50][51]. Proton-conducting nanoparticles are infiltrated into the anode and distributed over the Ni particles. These proton-conducting nanoparticles with basic surface can absorb and dissociate water, as abovementioned, which subsequently react with deposited carbon or sulfur; thus, this approach alleviates coking and sulfur poisoning. For example, the peak power density of direct-methane SOFCs at 650 °C was improved from 0.62 W cm⁻² to 1.27 W cm⁻² after decorating the Ni-GDC anode with BCY particles, indicative of the bifunctionality of proton-conducting oxides [50].

References

- Lelieveld, J.; Klingmüller, K.; Pozzer, A.; Burnett, R.T.; Haines, A.; Ramanathan, V. Effects of fossil fuel and total anthropogenic emission removal on public health and climate. *Proc. Natl. Acad. Sci. USA* 2019, 116, 7192.
- Feng, Y.; Luo, J.; Chuang, K.T. Propane Dehydrogenation in a Proton-conducting Fuel Cell. *J. Phys. Chem. C* 2008, 112, 9943–9949.
- Abdelkareem, M.A.; Elsaid, K.; Wilberforce, T.; Kamil, M.; Sayed, E.T.; Olabi, A. Environmental aspects of fuel cells: A review. *Sci. Total Environ.* 2021, 752, 141803.
- O'hayre, R.; Cha, S.-W.; Colella, W.; Prinz, F.B. *Fuel Cell Fundamentals*; John Wiley & Sons: Hoboken, NJ, USA, 2016.
- Abdalla, A.M.; Hossain, S.; Petra, P.M.; Ghasemi, M.; Azad, A.K. Achievements and trends of solid oxide fuel cells in clean energy field: A perspective review. *Front. Energy* 2020, 14, 359–382.
- Steele, B.C.H.; Heinzel, A. Materials for fuel-cell technologies. *Nature* 2001, 414, 345–352.
- McIntosh, S.; Gorte, R.J. Direct Hydrocarbon Solid Oxide Fuel Cells. *Chem. Rev.* 2004, 104, 4845–4866.
- Yue, W.; Li, Y.; Zheng, Y.; Wu, T.; Zhao, C.; Zhao, J.; Geng, G.; Zhang, W.; Chen, J.; Zhu, J.; et al. Enhancing coking resistance of Ni/YSZ electrodes: In situ characterization, mechanism research, and surface engineering. *Nano Energy* 2019, 62, 64–78.
- Viinikainen, T.; Rönkkönen, H.; Bradshaw, H.; Stephenson, H.; Airaksinen, S.; Reinikainen, M.; Simell, P.; Krause, O. Acidic and basic surface sites of zirconia-based biomass gasification gas clean-up catalysts. *Appl. Catal. A Gen.* 2009, 362, 169–177.
- Boldrin, P.; Ruiz-Trejo, E.; Mermelstein, J.; Bermúdez Menéndez, J.M.; Ramírez Reina, T.; Brandon, N.P. Strategies for Carbon and Sulfur Tolerant Solid Oxide Fuel Cell Materials, Incorporating Lessons from Heterogeneous Catalysis. *Chem. Rev.* 2016, 116, 13633–13684.
- Skaftø, T.L.; Blennow, P.; Hjelm, J.; Graves, C. Carbon deposition and sulfur poisoning during CO₂ electrolysis in nickel-based solid oxide cell electrodes. *J. Power Sources* 2018, 373, 54–60.
- Wei, K.; Wang, X.; Budiman, R.A.; Kang, J.; Lin, B.; Zhou, F.; Ling, Y. Progress in Ni-based anode materials for direct hydrocarbon solid oxide fuel cells. *J. Mater. Sci.* 2018, 53, 8747–8765.
- Wang, W.; Qu, J.; Julião, P.S.B.; Shao, Z. Recent Advances in the Development of Anode Materials for Solid Oxide Fuel Cells Utilizing Liquid Oxygenated Hydrocarbon Fuels: A Mini Review. *Energy Technol.* 2019, 7, 33–44.
- Da Silva, F.S.; de Souza, T.M. Novel materials for solid oxide fuel cell technologies: A literature review. *Int. J. Hydrogen Energy* 2017, 42, 26020–26036.
- Iwahara, H.; Uchida, H.; Ono, K.; Ogaki, K. Proton Conduction in Sintered Oxides Based on BaCeO₃. *J. Electrochem. Soc.* 1988, 135, 529–533.

16. Katahira, K.; Kohchi, Y.; Shimura, T.; Iwahara, H. Protonic conduction in Zr-substituted BaCeO₃. *Solid State Ion.* 2000, 138, 91–98.
17. Zuo, C.; Zha, S.; Liu, M.; Hatano, M.; Uchiyama, M. Ba(Zr_{0.1}Ce_{0.7}Y_{0.2})O_{3-δ} as an Electrolyte for Low-Temperature Solid-Oxide Fuel Cells. *Adv. Mater.* 2006, 18, 3318–3320.
18. Yang, L.; Wang, S.; Blinn, K.; Liu, M.; Liu, Z.; Cheng, Z.; Liu, M. Enhanced Sulfur and Coking Tolerance of a Mixed Ion Conductor for SOFCs: BaZr_{0.1}Ce_{0.7}Y_{0.2-x}O_{3-δ}. *Science* 2009, 326, 126.
19. Choi, S.; Kucharczyk, C.J.; Liang, Y.; Zhang, X.; Takeuchi, I.; Ji, H.-I.; Haile, S.M. Exceptional power density and stability at intermediate temperatures in protonic ceramic fuel cells. *Nat. Energy* 2018, 3, 202–210.
20. Duan, C.; Kee, R.J.; Zhu, H.; Karakaya, C.; Chen, Y.; Ricote, S.; Jarry, A.; Crumlin, E.J.; Hook, D.; Braun, R.; et al. Highly durable, coking and sulfur tolerant, fuel-flexible protonic ceramic fuel cells. *Nature* 2018, 557, 217–222.
21. Fabbri, E.; Pergolesi, D.; Traversa, E. Materials challenges toward proton-conducting oxide fuel cells: A critical review. *Chem. Soc. Rev.* 2010, 39, 4355–4369.
22. Duan, C.; Tong, J.; Shang, M.; Nikodemski, S.; Sanders, M.; Ricote, S.; Almansoori, A.; O'Hayre, R. Readily processed protonic ceramic fuel cells with high performance at low temperatures. *Science* 2015, 349, 1321.
23. Mogensen, M.; Kammer, K. Conversion of Hydrocarbons in Solid Oxide Fuel Cells. *Annu. Rev. Mater. Res.* 2003, 33, 321–331.
24. Kee, R.J.; Zhu, H.; Goodwin, D.G. Solid-oxide fuel cells with hydrocarbon fuels. *Proc. Combust. Inst.* 2005, 30, 2379–2404.
25. Ge, X.-M.; Chan, S.-H.; Liu, Q.-L.; Sun, Q. Solid Oxide Fuel Cell Anode Materials for Direct Hydrocarbon Utilization. *Adv. Energy Mater.* 2012, 2, 1156–1181.
26. Saadabadi, S.A.; Thallam Thattai, A.; Fan, L.; Lindeboom, R.E.F.; Spanjers, H.; Aravind, P.V. Solid Oxide Fuel Cells fuelled with biogas: Potential and constraints. *Renew. Energy* 2019, 134, 194–214.
27. Mohammed, H.; Al-Othman, A.; Nancarrow, P.; Tawalbeh, M.; El Haj Assad, M. Direct hydrocarbon fuel cells: A promising technology for improving energy efficiency. *Energy* 2019, 172, 207–219.
28. Gür, T.M. Comprehensive review of methane conversion in solid oxide fuel cells: Prospects for efficient electricity generation from natural gas. *Prog. Energy Combust. Sci.* 2016, 54, 1–64.
29. Wang, W.; Su, C.; Wu, Y.; Ran, R.; Shao, Z. Progress in Solid Oxide Fuel Cells with Nickel-Based Anodes Operating on Methane and Related Fuels. *Chem. Rev.* 2013, 113, 8104–8151.
30. Meng, Y.; Gao, J.; Zhao, Z.; Amoroso, J.; Tong, J.; Brinkman, K.S. Review: Recent progress in low-temperature proton-conducting ceramics. *J. Mater. Sci.* 2019, 54, 9291–9312.
31. Fabbri, E.; Bi, L.; Pergolesi, D.; Traversa, E. Towards the Next Generation of Solid Oxide Fuel Cells Operating Below 600 °C with Chemically Stable Proton-Conducting Electrolytes. *Adv. Mater.* 2012, 24, 195–208.
32. Duan, C.; Huang, J.; Sullivan, N.; O'Hayre, R. Proton-conducting oxides for energy conversion and storage. *Appl. Phys. Rev.* 2020, 7, 011314.
33. Konwar, D.; Nguyen, N.T.Q.; Yoon, H.H. Evaluation of BaZr_{0.1}Ce_{0.7}Y_{0.2}O_{3-δ} electrolyte prepared by carbonate precipitation for a mixed ion-conducting SOFC. *Int. J. Hydrogen Energy* 2015, 40, 11651–11658.
34. Chen, Y.; deGlee, B.; Tang, Y.; Wang, Z.; Zhao, B.; Wei, Y.; Zhang, L.; Yoo, S.; Pei, K.; Kim, J.H.; et al. A robust fuel cell operated on nearly dry methane at 500 °C enabled by synergistic thermal catalysis and electrocatalysis. *Nat. Energy* 2018, 3, 1042–1050.
35. Ormerod, R.M. Solid oxide fuel cells. *Chem. Soc. Rev.* 2003, 32, 17–28.
36. Takeguchi, T.; Kani, Y.; Yano, T.; Kikuchi, R.; Eguchi, K.; Tsujimoto, K.; Uchida, Y.; Ueno, A.; Omoshiki, K.; Aizawa, M. Study on steam reforming of CH₄ and C₂ hydrocarbons and carbon deposition on Ni-YSZ cermets. *J. Power Sources* 2002, 112, 588–595.
37. Yang, L.; Choi, Y.; Qin, W.; Chen, H.; Blinn, K.; Liu, M.; Liu, P.; Bai, J.; Tyson, T.A.; Liu, M. Promotion of water-mediated carbon removal by nanostructured barium oxide/nickel interfaces in solid oxide fuel cells. *Nat. Commun.* 2011, 2, 357.
38. Li, X.; Liu, M.; Lai, S.Y.; Ding, D.; Gong, M.; Lee, J.-P.; Blinn, K.S.; Bu, Y.; Wang, Z.; Bottomley, L.A.; et al. In Situ Probing of the Mechanisms of Coking Resistance on Catalyst-Modified Anodes for Solid Oxide Fuel Cells. *Chem. Mater.* 2015, 27, 822–828.
39. Hua, B.; Yan, N.; Li, M.; Sun, Y.-F.; Zhang, Y.-Q.; Li, J.; Etsell, T.; Sarkar, P.; Luo, J.-L. Anode-Engineered Protonic Ceramic Fuel Cell with Excellent Performance and Fuel Compatibility. *Adv. Mater.* 2016, 28, 8922–8926.

40. Wang, W.; Chen, Y.; Wang, F.; Tade, M.O.; Shao, Z. Enhanced electrochemical performance, water storage capability and coking resistance of a Ni+BaZr_{0.1}Ce_{0.7}Y_{0.1}Yb_{0.1}O_{3-δ} anode for solid oxide fuel cells operating on ethanol. *Chem. Eng. Sci.* 2015, 126, 22–31.
41. Marrony, M. *Proton-Conducting Ceramics: From Fundamentals to Applied Research*; CRC Press: Boca Raton, FL, USA, 2015.
42. Zhu, H.; Braun, R.J.; Kee, R.J. Thermodynamic Analysis of Energy Efficiency and Fuel Utilization in Protonic-Ceramic Fuel Cells with Planar Co-Flow Configurations. *J. Electrochem. Soc.* 2018, 165, F942–F950.
43. Duan, C.; Kee, R.; Zhu, H.; Sullivan, N.; Zhu, L.; Bian, L.; Jennings, D.; O'Hayre, R. Highly efficient reversible protonic ceramic electrochemical cells for power generation and fuel production. *Nat. Energy* 2019, 4, 230–240.
44. Coors, W.G. Protonic ceramic fuel cells for high-efficiency operation with methane. *J. Power Sources* 2003, 118, 150–156.
45. Feng, Y.; Luo, J.-L.; Chuang, K.T. Carbon deposition during propane dehydrogenation in a fuel cell. *J. Power Sources* 2007, 167, 486–490.
46. Liu, S.; Chuang, K.T.; Luo, J.-L. Double-Layered Perovskite Anode with in Situ Exsolution of a Co–Fe Alloy To Cogenerate Ethylene and Electricity in a Proton-Conducting Ethane Fuel Cell. *ACS Catal.* 2016, 6, 760–768.
47. Hua, B.; Yan, N.; Li, M.; Zhang, Y.-Q.; Sun, Y.-F.; Li, J.; Etsell, T.; Sarkar, P.; Chuang, K.; Luo, J.-L. Novel layered solid oxide fuel cells with multiple-twinned Ni_{0.8}Co_{0.2} nanoparticles: The key to thermally independent CO₂ utilization and power-chemical cogeneration. *Energy Environ. Sci.* 2016, 9, 207–215.
48. Konwar, D.; Park, B.J.; Basumatary, P.; Yoon, H.H. Enhanced performance of solid oxide fuel cells using BaZr_{0.2}Ce_{0.7}Y_{0.1}O_{3-δ} thin films. *J. Power Sources* 2017, 353, 254–259.
49. Lei, L.; Keels, J.M.; Tao, Z.; Zhang, J.; Chen, F. Thermodynamic and experimental assessment of proton conducting solid oxide fuel cells with internal methane steam reforming. *Appl. Energy* 2018, 224, 280–288.
50. Li, M.; Hua, B.; Luo, J.-L.; Jiang, S.P.; Pu, J.; Chi, B.; Li, J. Enhancing Sulfur Tolerance of Ni-Based Cermet Anodes of Solid Oxide Fuel Cells by Ytterbium-Doped Barium Cerate Infiltration. *ACS Appl. Mater. Interfaces* 2016, 8, 10293–10301.
51. Li, M.; Hua, B.; Luo, J.-L.; Jiang, S.P.; Pu, J.; Chi, B.; Jian, L. Carbon-tolerant Ni-based cermet anodes modified by proton conducting yttrium- and ytterbium-doped barium cerates for direct methane solid oxide fuel cells. *J. Mater. Chem. A* 2015, 3, 21609–21617.

Retrieved from <https://encyclopedia.pub/entry/history/show/24090>